Time-clustering of wave storms in the Mediterranean Sea

Giovanni Besio[1], Riccardo Briganti[2], Alessandro Romano[3], Lorenzo Mentaschi[4], and Paolo De Girolamo[3]

[1]Department of Civil, Chemical and Environmental Engineering, University of Genoa, Italy
[2]Department of Civil Engineering, University of Nottingham, UK
[3]Department of Civil, Architectural and Environmental Engineering, La Sapienza University, Rome, Italy
[4]European Commission, Joint Research Centre (JRC), Ispra, Italy

Correspondence to: Giovanni Besio (giovanni.besio@unige.it)

Abstract. In this contribution we identify storm time-clustering in the Mediterranean Sea through the analysis of the spatial distribution of the Allan Factor. This parameter is evaluated from long time series of wave height provided by means of oceanographic buoy measurements and hindcast re-analysis spanning in the period 1979-2014 and characterized by a horizontal resolution of about 0.1 degree in longitude and latitude and a temporal sampling of one hour (Mentaschi et al., 2015). Results

5   reveal clustering mainly for two distinct ranges of time scales. The first range of time scales (12 hrs to 50 days) is associated to sequences of storms generated by the persistence of the same meteorological system. The second range, associated to timescales between 50 and 100 days, reveals seasonal fluctuations. Transitional regimes are present at some locations in the basin. The spatial distribution of the Allan Factor reveals that the clustering at smaller time scales is present in the North-West of the Mediterranean, while clustering at larger scales is observed in the whole basin. This analysis is believed to be important

10   to assess the local increased flood and coastal erosion risks due to storm clustering.

1   Introduction

In recent years the occurring of different storms in a short time has been studied in the context of storm driven erosion of beaches and dunes. Indeed it has been showed by different authors (Coco et al., 2014, Splinter et al., 2014; Karunarathna et al., 2014; Dissanayake et al., 2015) that storms occurring in quick succession may result in greater beach erosion than the cumulated

15   erosion induced by single storms of far higher return periods.

In the events analysed in the aforementioned studies both the surge and the wave components played an important role. While studies that identify time-clustering of storm surges are available (e.g. Wadey et al., 2014), there is no study, to the best knowledge of the authors, that analyses the clustering properties of wave storms alone. In micro-tidal environments, such as the Mediterranean Sea, wave storms are the principal driver of short term coastal erosion and flooding, hence it is important to

20   understand the occurrence of clustering. The Mediterranean Sea wave climate has been extensively studied (e.g. Sartini et al., 2015a) and it is known that throughout the basin winter is richer in cyclones and, in turn, in wave storms. However, regional differences are significant. Sartini et al. (2015a) linked the seasonality of wave storms to seasonal features of atmospheric

pressure over the Mediterranean basin strongly suggesting that the local typical meteorological conditions determine time regimes of storm waves.

The present work addresses the gap in the knowledge of the occurrence of time-clustering of wave storms by carrying out an analysis of wave storms sequences using the Allan Factor (hereinafter AF, Allan, 1966; Barnes and Allan, 1966), a

5   well established technique to study the time behaviour of environmental processes. The AF of a specific sequence of events shows a power-law behaviour if the underlying process is characterised by clustering in the time scales studied. The simplicity of the AF analysis made it popular in the study of time sequences of a number of physical processes such as earthquakes (Telesca et al., 2002), lightning (Telesca et al., 2008), rainfall (Telesca et al., 2007) or fires (Telesca and Pereira, 2010). Here we identify storm time-clustering in the Mediterranean Sea through the analysis of the AF evaluated on long time series of wave

10 height provided by hindcast re-analysis spanning the period 1979-2014 (Mentaschi et al., 2015). This analysis is validated and compared against the AF evaluated using the time series of wave measurements of the Italian national Sea Wave Measurement Network (Rete Ondametrica Nazionale, hereinafter RON). The objective of this study is to identify the presence of time-clustering of wave storms in the whole Mediterranean basin and examine the time scales at which events are correlated as well as the spatial distribution of the clustering. To this end we identify scaling properties of wave storms in the wave hindcast

15 database and map them over the Mediterranean Sea. The paper is organised as follows: after this Introduction, Section 2 explains the methodology used for the AF analysis, Section 3 describes the datasets used, Section 4 illustrates the results and Section 5 discusses the results and draws the conclusions of this work.

2   Clustering analysis methodology

Sequences of natural events such as earthquakes, rainfall, wildfires, can be seen as realisations of stochastic point processes.

20 A process of this kind describes events that occur randomly in time and it is completely defined by the times at which these events occur. Here time series of sea states are considered. Each sea state is defined by a set of spectral parameter, such as the significant wave height H_s, the peak period T_p, the mean period $T_{m-1,0}$ and the mean direction of propagation θ_m. Waves are always present on the sea surface, hence a sequence of storms need to be extracted from a time series of sea states by considering only events that satisfy a certain criterion. A storm is commonly defined as a sequence of sea states in which H_s

25 exceeds a given threshold (e.g. Goda, 1988). In this work, a threshold for each node is defined by considering the local 98% percentile of the H_s distribution, regardless of θ_m (omnidirectional analysis, see figure 1 for threshold values of H_s obtained with the hindcast model used here). The time t_i at which the threshold is exceeded for the first time in each storm defines the event as part of a point process. If the interval between two subsequent events is below 12 hours, the two are regarded as one event, this is common practice in analysing storms and the value is deemed appropriate for the Mediterranean Sea

30 (e.g. Sartini et al., 2015a). Therefore, in each of the computational nodes over the Mediterranean Sea (see figure 2 for a map of the domain and the location of few control grid points used in this study to show the single point behavior of the AF), a point process is defined. An example for the control point A and for the years 2004 and 2005, is given in figure 3. In this figure it is evident that most of the storms, during the two years considered, occur between November and May, showing the
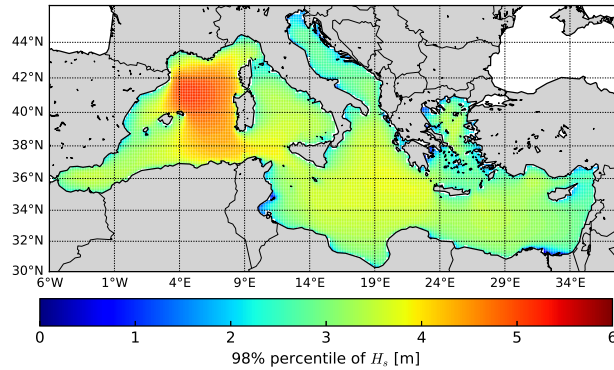
Figure 1. Value of significant wave height threshold in meters for the 98% percentile
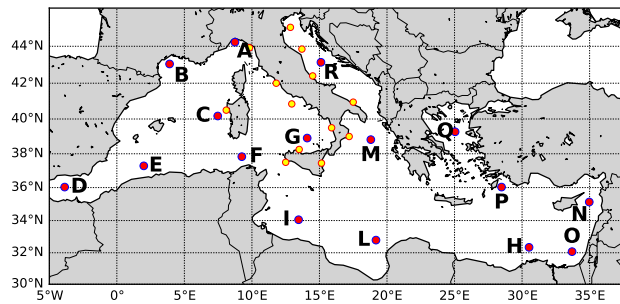
Figure 2. Hindcast control grid points (red circle) and RON buoys reference points (yellow circles)

pronounced seasonality that characterizes the basin. Figure 4 shows the number of events defined in each month over the year in the hindcast record for the same reference point A during the period 1979-2014 as a function of the percentile threshold (different wave heights. The seasonal variability of the storms in the Mediterranean basin is again recognizable. Note that the difference in number of storms between the different percentiles considered is maximum in the most active months and, if the

5   99% is chosen, the differences among seasons are small, although the seasonal variability is still recognizable.

Each of these processes is studied by defining equally spaced time windows of duration τ and counting the events in each window. The result is a sequence of counts N_k ($k = 1, .., M$, where M is the number of time windows). The clustering of the events is then studied with the Allan Factor (Allan, 1966; Barnes and Allan, 1966), defined as the variance of successive counts as:

10   $$\mathrm{AF}\left(\tau\right) = \frac{\left\langle \left[N_{k+1}\left(\tau\right) - N_k\left(\tau\right)\right]^2 \right\rangle}{\left\langle N_k\left(\tau\right)\right\rangle} \tag{1}$$

In general term, a point process is called fractal when a number of the relevant statistics shows scaling with related scaling exponents (Lowen and Teich, 1995). This implies that the AF depends from τ with a power-law, with exponent α, which
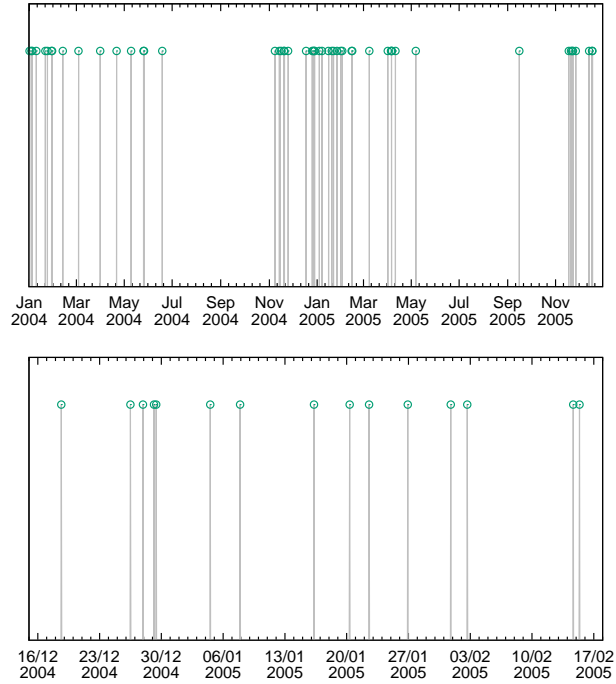
Figure 3. Storm occurence for the Northern Thyrrenian reference point (A): 2004/2005, top panel; zoom on winter 2004/2005, bottom panel
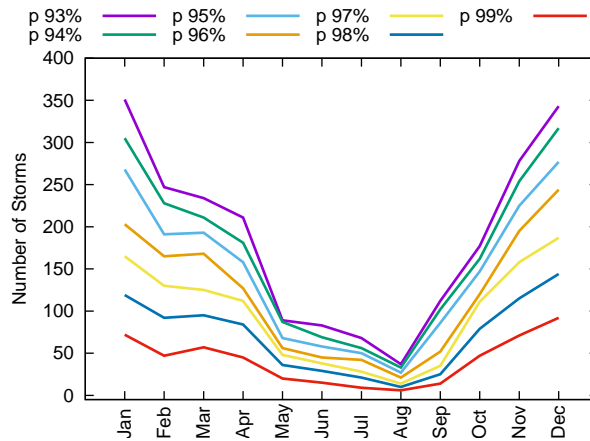
Figure 4. Number of Storms vs Threshold for the Northern Thyrrenian reference point (A)

indicates the presence of clusters of points over a number of time scales τ. For a fractal process with $0 < \alpha < 3$ this power law reads (Telesca and Pereira, 2010):

$$\mathrm{AF}(\tau) = 1 + \left(\frac{\tau}{\tau_1}\right)^{\alpha} \tag{2}$$

where τ_1 is the fractal onset time that marks the lower limit for significant scaling behavior for the AF. For times smaller than τ_1 there is no significant time correlation, while for times greater than τ_1 a characteristic fractal trend can be derived from the value of the exponent. If the storms process is Poissonian, the arrival times are uncorrelated, hence α is expected to be zero and the AF will be near of below unity. If clusters are present over a significant range of time scales it will be possible to identify

5    $\alpha > 0$ and AF> 1. In the present work α is estimated by the slope of the curve of the AF as a function of τ. Note different ranges of τ can reveal different time scaling (clustering) of the same process through different slopes of eq. (2) due to different kind of forcing (Telesca and Pereira, 2010).

3   Wave data

3.1   Wave hindcast

10   Wave hindcast in the Mediterranean Sea has been implemented on a time window covering 36 years, from the first of January of 1979 till the 31st of December of 2014 (www.dicca.unige.it/meteocean/hindcast.html). The wave model is forced by the 10-m wind fields obtained by means of the non-hydrostatic model WRF-ARW (Weather Research and Forecasting - Advanced Research WRF) version 3.3.1 (Skamarock et al., 2008). In the present study a Lambert conformal grid covering the whole Mediterranean Sea with a resolution of about 0.1 degree in longitude and latitude has been used. Initial and boundary conditions

15   for atmospheric simulations were provided from the CFSR (Climate Forecast System Reanalysis) database (Saha et al., 2010). Use of CFSR reanalysis data for wave modeling provides reliable results, even if sometimes extreme wave conditions are not properly modeled (Cavaleri, 2009; Cox et al., 2011; Splinder et al., 2011; Carvalho et al., 2012; Chawla et al., 2013). For further details of the set-up and validation of the meteorological model readers can refer to Cassola et al. (2015, 2016).

    Generation and propagation of sea waves have been modeled using WavewatchIII®, version 3.14 (Tolman, 2009). A 336x180

20   regular grid covers the whole Mediterranean Sea with a resolution of 0.1273×0.09 degrees, corresponding to about $10km$ at the latitude of $45°$N. Spectral resolution is characterized by 24 bins in direction and 25 frequencies ranging from 0.06 to $0.7Hz$ with a step factor of 1.1. The output has been recorded hourly in all points of the computation grid for integrated quantities (i.e. significant wave height H_s, mean period $T_{m-1,0}$, peak period T_p, mean direction θ_m, peak direction θ_p, direction spreading $\Delta\theta$). The validation of the wave hindcast has been carried out through extensive comparison of simulated quantities and wave

25   buoy data (cfr. Mentaschi et al., 2013a, b, 2015) and has already been employed for different applications such as wave energy resource assessment (Besio et al., 2016) and extreme and wave climate analysis (Sartini et al., 2015a, b).

3.2   Buoy data

The Italian Sea Wave Measurement Network (Rete Ondametrica Nazionale RON) started operating in July 1989 (De Boni et al., 1992; Arena et al., 2001; Corsini et al., 2004). Until 1998 the network was made by eight pitch-roll directional buoys located

30   offshore, in deep water conditions, of several sea areas equally spaced along the italian peninsula. These original eight stations were: La Spezia, Alghero, Ortona, Ponza, Monopoli, Crotone, Catania and Mazara del Vallo. The statistical wave parame-

ters (i.e. significant wave height H_s, mean period T_m, peak period T_p, mean direction θ_m) were originally retrieved every three-hours, below a station-dependent threshold for H_s, and every half an hour above this threshold. Between 1999 and 2002 substantial changes in terms of instruments, management and data recording protocols, have been enforced to the RON network. New buoys were deployed (i.e. Cetraro, Ancona, Capo Comino, Civitavecchia, Capo Gallo and Punta della Maestra).

5 Furthermore, the data recording protocols have been changed to ensure half-hourly time series. The wave data time series, measured by the RON buoys, that have been analysed in the present study, cover a time window of 20 years, from the summer of 1989 until the spring of 2008 for the original eight buoys. As far as the newer buoys are considered, it is worth noting that the wave data time series measured by both the Ancona and Cetraro stations cover a shorter time window of 10 years, between 1999 and 2008, while only 5 years of wave measurements are available for both the Civitavecchia and Capo Gallo (Palermo)

10 stations. For the cluster analysis performed using the RON records, data every three hours were considered for all the stations.

4 Results

4.1 Comparison between hindcast and buoy measurements

In order to assess the reliability of the hindcast time series related to storm cluster analysis, the results of AF for the RON buoys will be analysed and compared to the corresponding grid points of the hindcast model. These results are shown in figures 5-

15 7. Results obtained on the basis of the RON data and hindcast series show a good qualitative and quantitative agreement especially for lower threshold conditions (98% percentile) while for higher threshold (99.5% percentile) tend to present stronger differences, e.g. in Alghero and Mazara (see figure 5) and Mazara (see figure 6). These findings can be explained by the fact that increasing the threshold limit would select just the most energetic wave conditions that are the most difficult to be reproduced by numerical models (a.o. Cavaleri, 2009) and sometime to be recorded by wave buoys (breakdown, damages or even loss of the

20 instrumentation). Differences are usually larger for smaller time scales, i.e. $0.5 < \tau < 50$ days and the exponent α attains values around $0.2 - 0.3$. For $\tau > 50$ days the variability is lower and all the curves show slopes of similar value, with $\alpha \simeq 1.1 - 1.2$ in average. These results confirm that the hindcast data and the wave buoys show very similar clustering properties.

In all cases, and consistently between model and data estimates, the AF is greater than one for τ greater than 12-24 hours and two distinct slopes are recognizable. The first slope is observed generally between 0.5 to 20-50 days in most of the stations. The

25 second, steeper, slope is observed generally between 50 and 100 days. Transition between the two slopes differs from station to station. In most stations there is a sharp discontinuity between the two slopes (e.g. Alghero, Ancona, Catania in figure 5). In some cases there is a plateau or a slight decrease in AF value at this discontinuity (e.g. in Palermo and Ponza in figure 7). In few cases a more gentle transition is seen (e.g. in Ortona, see figure 7) that occurs between 10 and 50 days. In all stations the AF decreases rapidly after 300 days, in correspondence with the annual cycle.
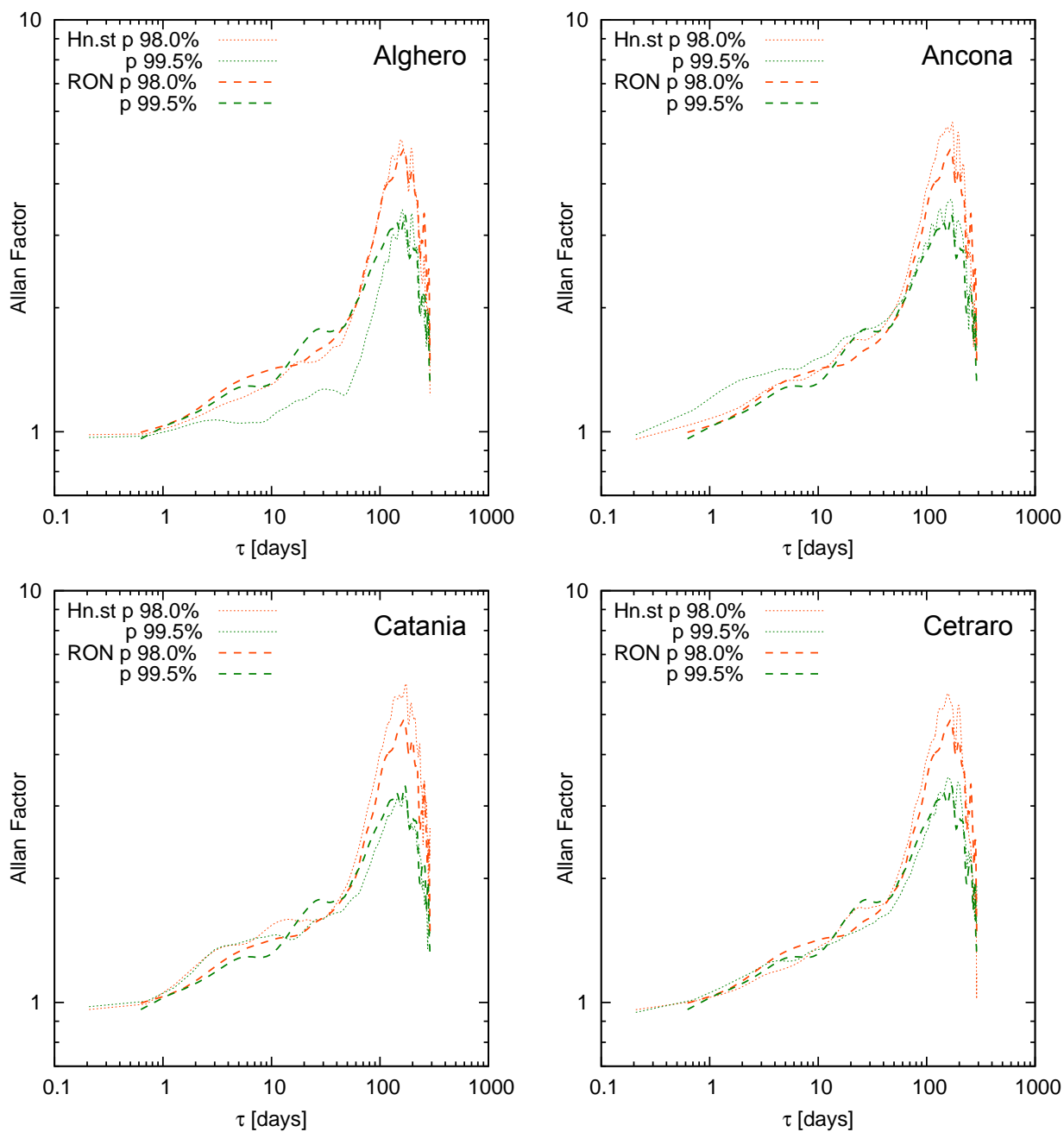
Figure 5. Comparison of Allan Factor between RON and Hindcast data series for different threshold percentiles (98% and 99.5%)
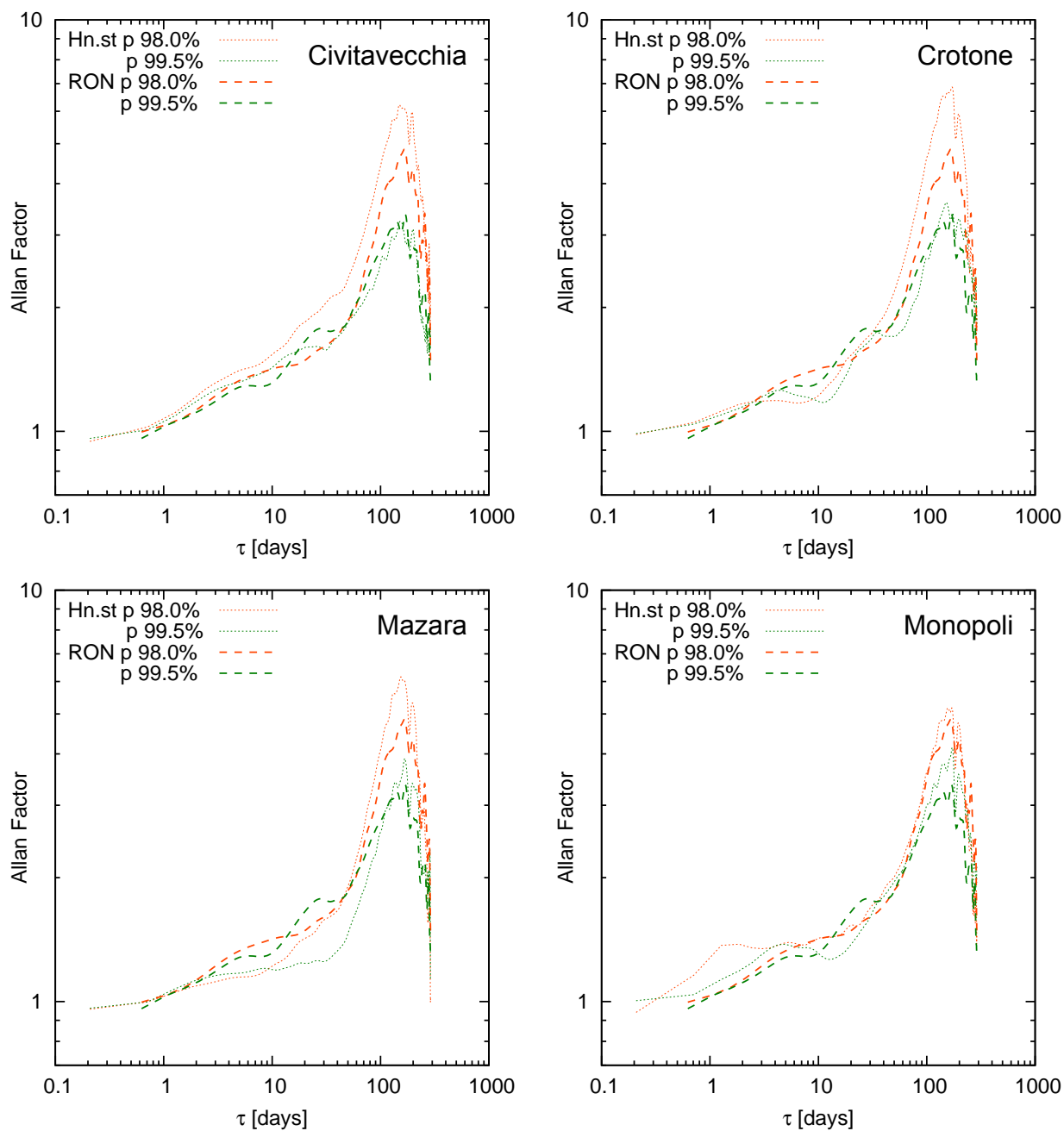
Figure 6. Comparison of Allan Factor between RON and Hindcast data series for different threshold percentiles (98% and 99.5%)
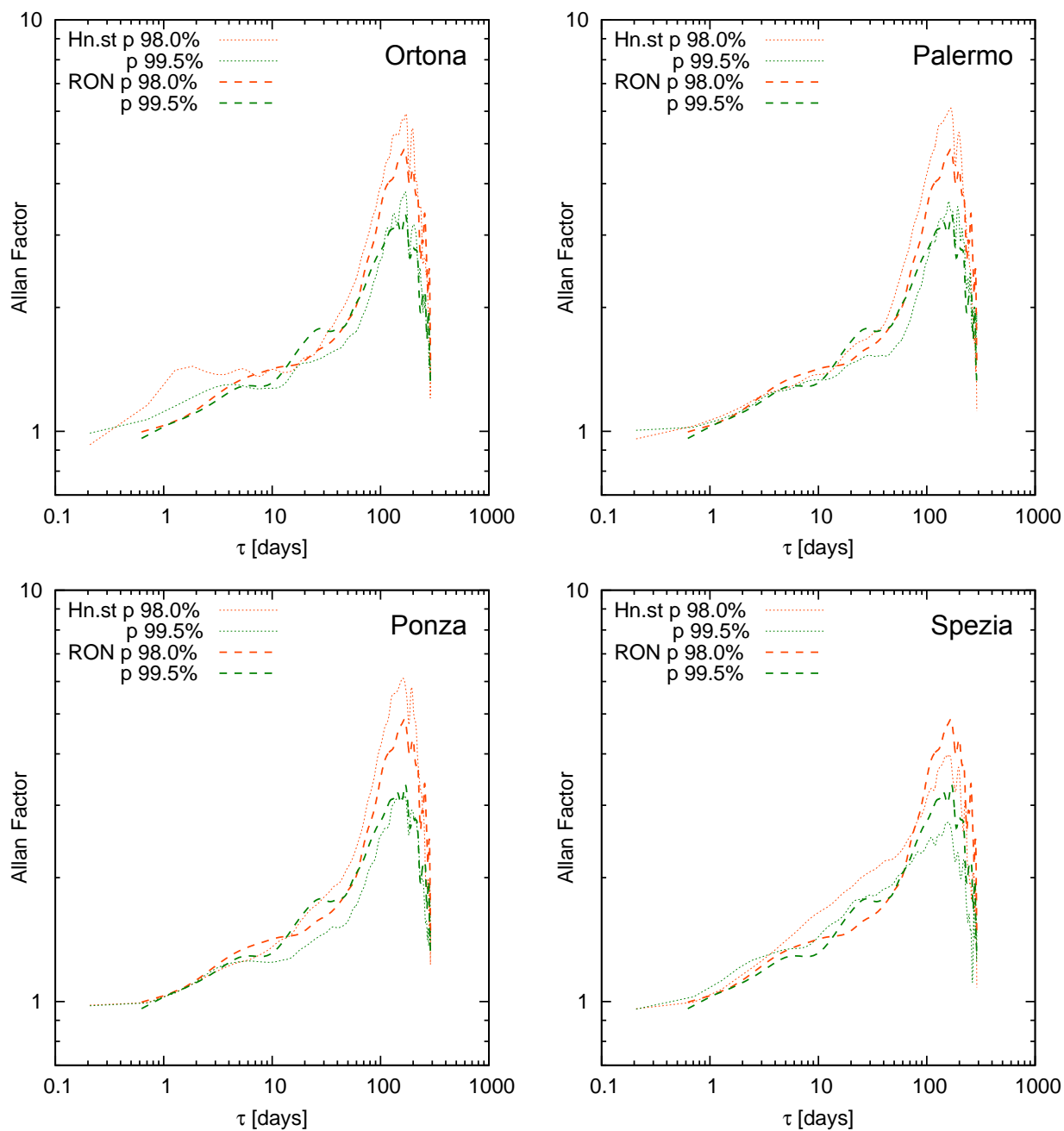
Figure 7. Comparison of Allan Factor between RON and Hindcast data series for different threshold percentiles (98% and 99.5%)

4.2 AF results over the Mediterranean Sea

Results from the control points located over the basin (see figure 2) are shown in figures 8-11. The AF curves reveal that the characteristics seen in the RON buoys are more general. In particular, three types of AF curves emerge:

a) the first type shows two distinct slopes with a slight decrease of AF between the two. Although the value of τ that marks

5   the separation between the two threshold varies in space, it can be seen that the change in slope occurs at around $\tau = 20$ days in most cases. This regime is similar to that seen at Ponza buoy and it is very evident at points A (North Thyrrenian Sea), B (Gulf of Lyon), D (Alboran Sea), and E (Algerian Sea) while is not observed for South-East Mediterranean points.

b) the second type shows three slopes, one for $\tau < 10$ days, one for $\tau > 50$ days, and a transition slope in between. The

10   slope for small values of τ varies, with α being higher at point R (Adriatic Sea) than elsewhere, e.g. points C (West Sardinia), F (Tunisian coast), G (South Thyrrenian Sea), M (Ionian Sea), Q (Aegean Sea). At some of these points, e.g. point Q, the small time-scales slope approaches $\alpha = 0$.

c) in the third type only one slope is clearly recognizable, generally for $\tau > 20$ days. At smaller scales α can be reasonably considered naught. This is the case of the southern Mediterranean points H (Egypt), I (Western Libia), L (North-East

15   Libia), O (South East Mediterranean Sea) and P (Southern Turkey).

A common characteristics of all control points is that α for larger scales shows little variability with the location (i.e. a strong clustering for long period is observed in the whole Mediterranean basin). Also, in all cases as the highest percentile is used α for the small time scales tends to zero.

The spatial distribution of the slopes for the small and large time-scales is shown in figure 12. This figure has been obtained

20 by determining the best fit value of α at different time scales. In order to take into account the local differences in determining the transition between slopes and the different regimes seen in the representative points, the slope for the small time-scales has been estimated using four different ranges of τ. Clustering in the range $12 < \tau < 72$ hours is presented in panel a) while for $12 < \tau < 120$ hours results are showed in panel b). Within this range the small-scale slope is higher in the North-West Mediterranean Sea and, in particular in the North Thyrrenian Sea and in the Balearic Sea. Here α reaches values up to 0.3.

25 Areas with α around 0.2 are present in the Adriatic Sea, on the Syrian and Lebanese coast and along the Tunisian coast. The effect of widening the range of τ is to decrease the best fit value of α. This effect reduces the regions that show α significantly higher than zero in particular in the Adriatic Sea and on the East Coast of Tunisia. When the interval $12 < \tau < 240$ hours is used (figure 12 panel c) the best fit of α is significantly higher than zero only in the North-West Mediterranean Sea with the average α around 0.2 and zones with $\alpha > 0$ are present in the East part of the Adriatic Sea and on the Syrian coast.

30 The range of τ for larger time scales is consistent in the whole domain considered when the interval $1200 > \tau > 2400$ hours is used for best fitting α (figure 12 panel d). Also, the spatial distribution of α for these time-scales is more uniform compared with the previous smaller ranges. $\alpha > 1.0$ is seen in most of the Mediterranean Sea, with peaks in the Levantine Basin, while it
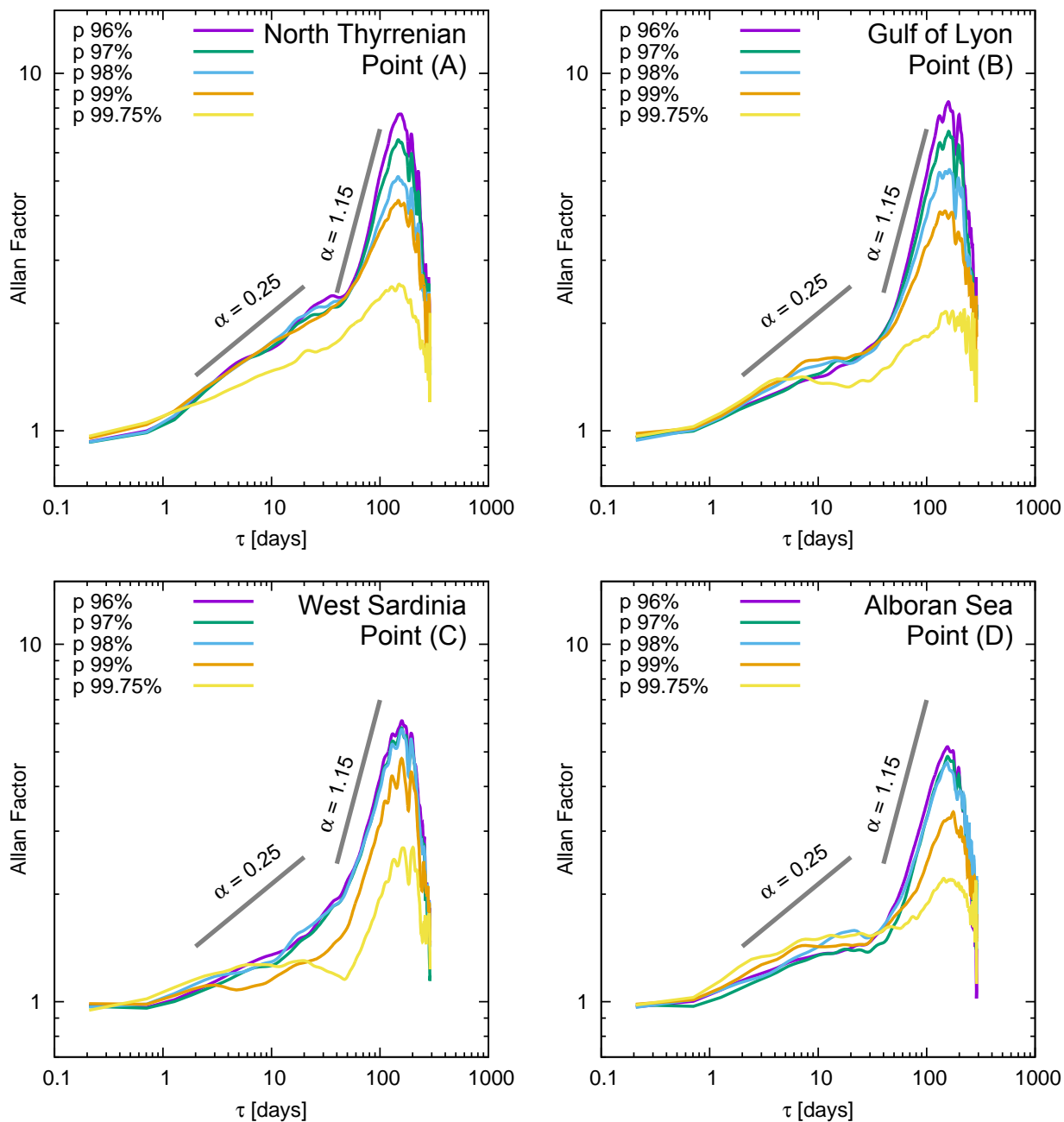
Figure 8. Allan Factor (AF) as a function of counting window τ and of the wave height threshold (different percentiles as in the legend) for different locations in the Mediterranean Sea (cfr. figure 2)
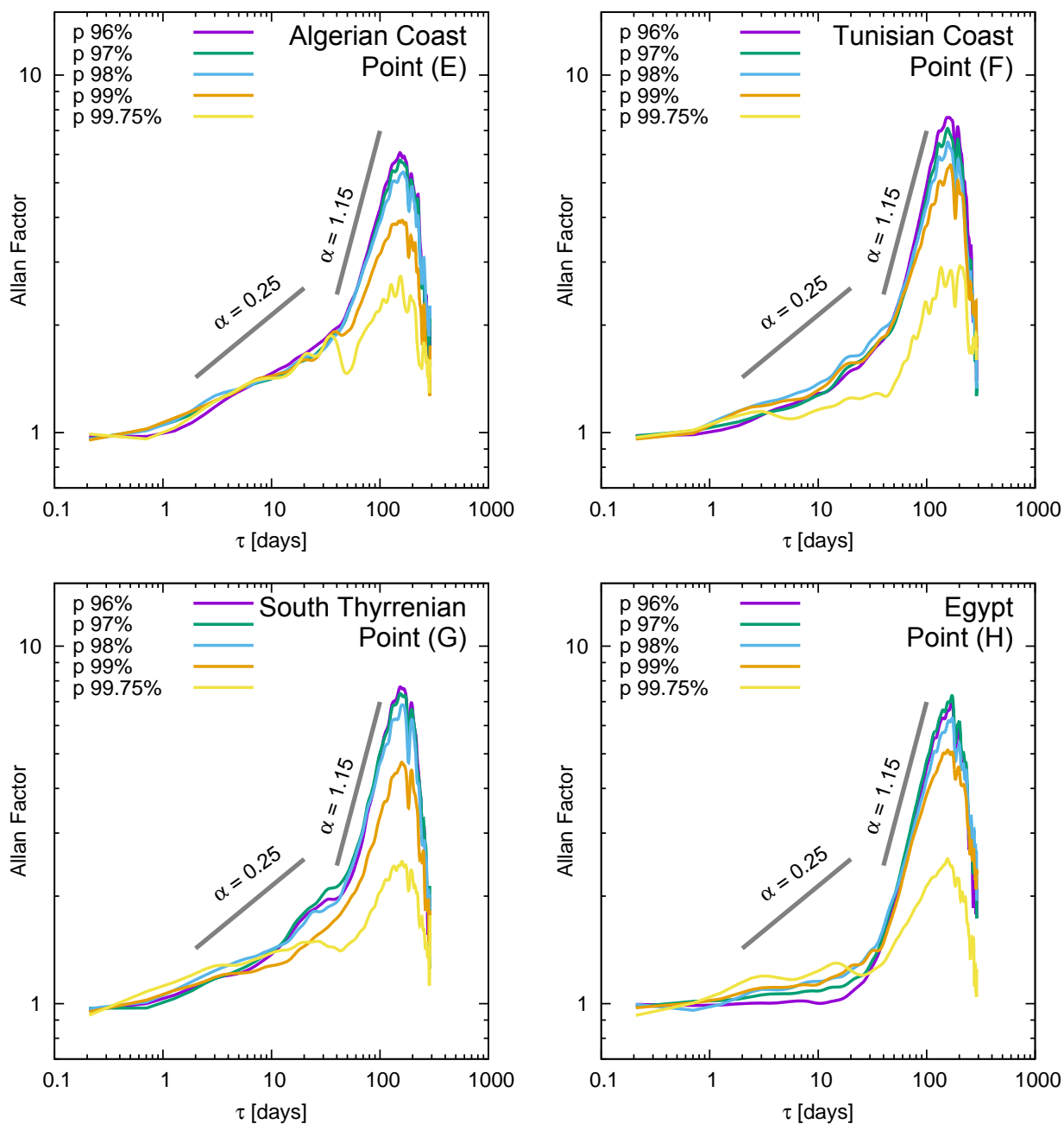
Figure 9. Allan Factor (AF) as a function of counting window τ and of the wave height threshold (different percentiles as in the legend) for different locations in the Mediterranean Sea (cfr. figure 2)
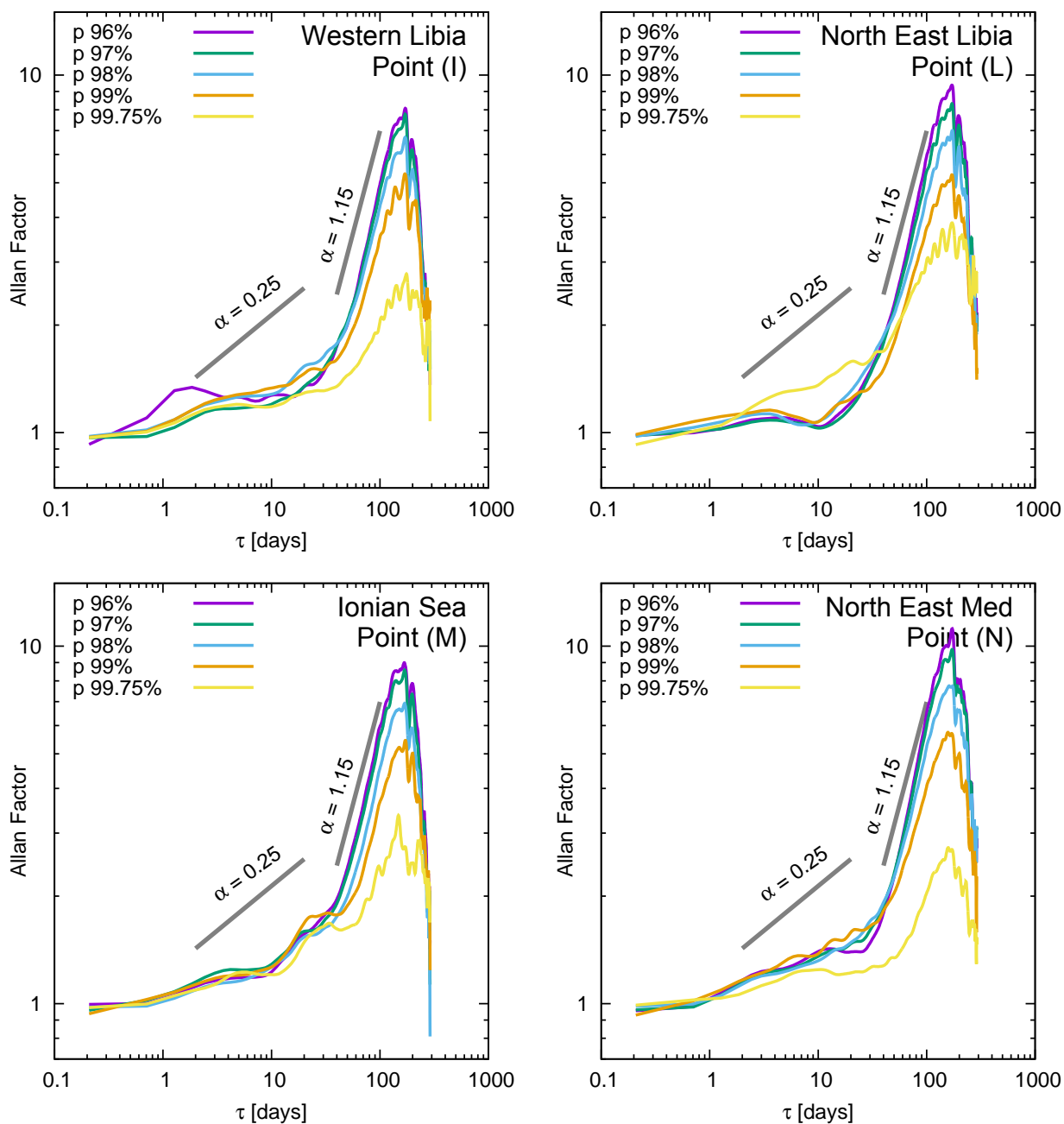
Figure 10. Allan Factor (AF) as a function of counting window τ and of the wave height threshold (different percentiles as in the legend) for different locations in the Mediterranean Sea (cfr. figure 2)
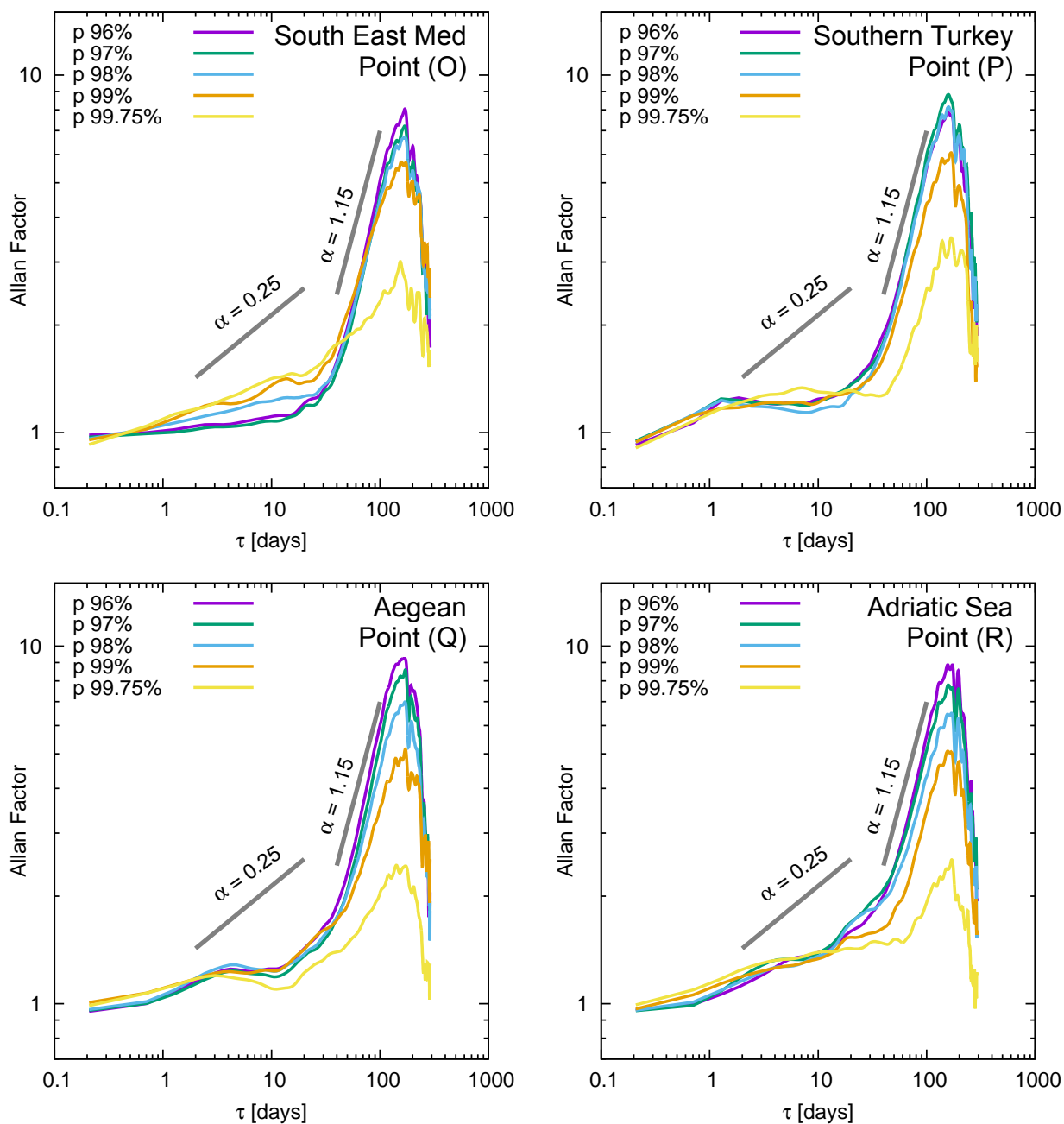
Figure 11. Allan Factor (AF) as a function of counting window τ and of the wave height threshold (different percentiles as in the legend) for different locations in the Mediterranean Sea (cfr. figure 2)
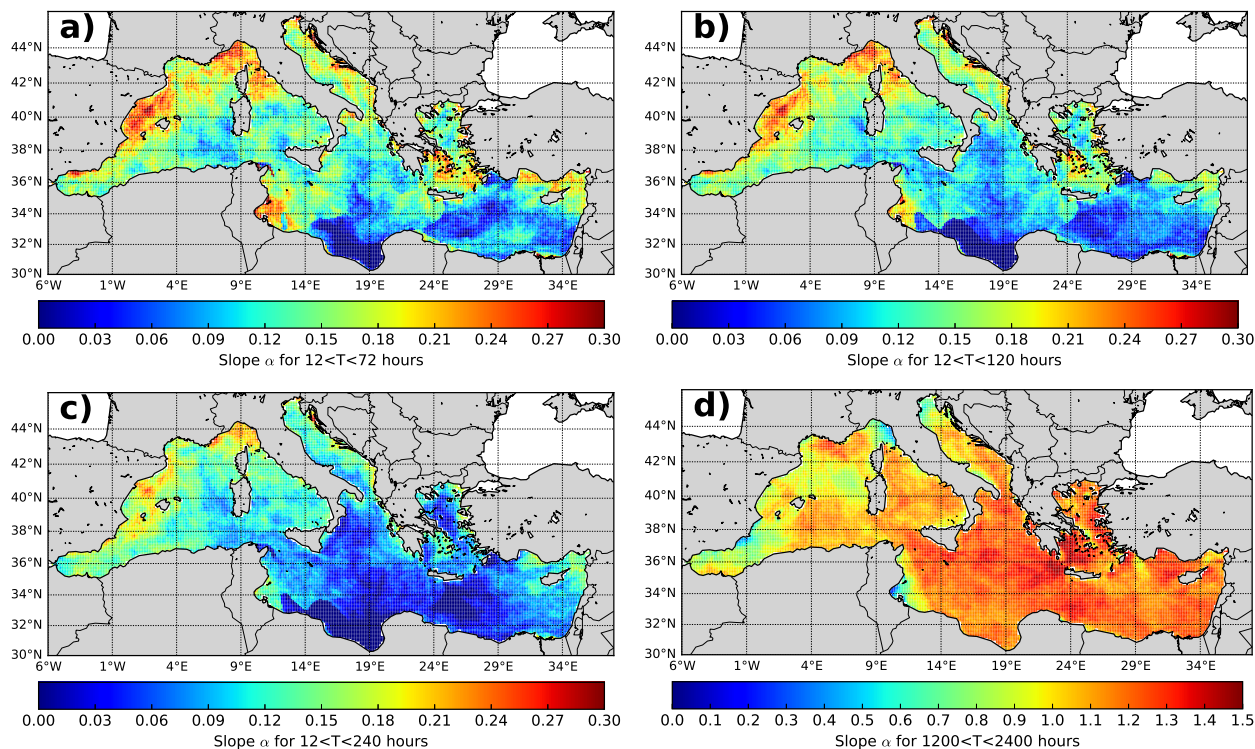
Figure 12. Spatial distribution of the fractal exponent α for the whole Mediterranean basin

becomes lower than unity only in the North Thyrrenian and Adriatic Seas and along the Southern Spain and Tunisia. The slope is larger in the Eastern than in the Western sub basins and it is maximum in the Aegean Sea.

5 Discussion and conclusions

The results presented above highlighted the presence of clustering (i.e. of AF>1) in the Mediterranean Sea. Two ranges of time

5   scales show very different value of the fractal dimension α. The behaviour between $1200 > \tau > 2400$ hours is explained with the intra-seasonal variability of the wave storms, which creates time-correlation of the meteorological forcings and, in turn, of the wave storms (basically the results reveal the summer-winter cycle). Similar scaling regimes have been observed in other phenomena with seasonal behaviour, e.g. fires (Telesca and Pereira, 2010). It is well known (Lionello et al., 2006, Sartini et al., 2015a) that the Mediterranean Sea is characterised by a very active winter, with the maximum wind speeds found in this season

10 throughout the basin. On the other hand summer shows the minimum wind intensity and storms are less frequent. Interestingly, although the exponent α is larger than unity in most of the basin, there are differences over the basin, with larger α seen in the South-Eastern Mediterranean. These results match with the findings by Sartini et al. (2015a), who found that the southern basin RON buoys (e.g. Crotone, in the Ionian Sea) showed higher seasonality than the Ponza and La Spezia buoy. The latter

is located in the Ligurian Sea, a region where α is lower. Although in the region the cyclogenesis in the Gulf of Genoa shows marked seasonality, cyclones are present throughout the year (Lionello et al., 2006, Sartini et al., 2015a) thus reducing the strength of the inter-seasonal clustering. The variability of the fractal dimension correlates well with the seasonal cycle of the Mediterranean cyclones as described by Lionello et al. (2016). In this study the Mediterranean is divided in four sectors, (see

5 figure 1 in Lionello et al., 2016). The South East sector, corresponding roughly with the Levantine Basin, is characterised by the highest variability due to the seasonal cycle, while the North West, corresponding to the Northern Thyrrenian Sea, The Gulf of Lyon and Belearic Sea is the most active sector in all seasons. This basin partitioning is revealed by AF results presented in figure 12 panel d).

This persistence of cyclonic events explains also the behaviour at smaller scales (i.e, $\tau < 1200$ hours), where the spatial

10 variability is more pronounced. In most of the Southern and Eastern Mediterranean the process is Poissonian at these scales, while clustering is found in the North-West of the Mediterranean Sea. Here local factors dominate in generating clustering. One example of this is the Gulf of Genoa, where cyclones are particularly frequent and, in average, the pressure is lower than other regions of the Thyrrenian Sea for most of the year (see figure 7 in Sartini et al., 2015a). The clustering at scales of days indicates that meterological conditions favour the occurrence of multiple events in few days. It is not a case that this behaviour

15 is seen in the most active cyclonic region of the Mediterranean Sea, e.g. the North West according to Lionello et al., 2016. Similar considerations apply to the North Adriatic Sea.

Clustering at these small time scales have the potential exacerbate local beach erosion generated by single storms, as shown in Dissanayake et al. (2015), hence it will be important to understand the implication of the found time regimes on the dynamics of the Mediterranean coastal regions.

20 *Author contributions.* G. Besio and L. Mentaschi developed the wave hindcast and the Allan Factor analysis for the Mediterranean Sea; R. Briganti coordinated the work and gave the theoretical ideas to develop the analysis; A. Romano developed the analysis for the RON buoy dataset. All the authors participated actively in the preparation and writing of the manuscript.

Acknowledgements. The work described in this publication was supported by the European Community's Horizon 2020 Research and Innovation Programme through the grant to HYDRALAB-PLUS, Contract no. 654110. R. Briganti expresses his gratitude to the Engi-

25 neering and Physical Sciences Research Council (EPSRC) for providing the funding through the FloodMEMORY project (Grant number: EP/K013513/1).

References

Allan, D. W.: Statistics of atomic frequency standards, Proceedings of the IEEE, 54, 221–230, 1966.

Arena, G., Briganti, R., Corsini, S., and Franco, L.: The Italian wave measurement buoy network: 12 years management experience, in: Proceedings of the waves 2001 conference, San Francisco, pp. 86–95, 2001.

5 Barnes, J. and Allan, D. W.: Statistics of atomic frequency standards, Proceedings of the IEEE, 54, 176–178, 1966.

Besio, G., Mentaschi, L., and Mazzino, A.: Wave energy resource assessment in the Mediterranean Sea on the basis of a 35-year hindcast, Energy, 94, 50–63, 2016.

Carvalho, D., Rocha, A., and Gomez-Gesteira, M.: Ocean surface wind simulation forced by different reanalyses: Comparison with observed data along the Iberian Peninsula coast, Ocean Modelling, 56, 31–42, 2012.

10 Cassola, F., Ferrari, F., and Mazzino, A.: Numerical simulations of Mediterranean heavy precipitation events with the WRF model: analysis of the sensitivity to resolution and microphysics parameterization schemes, Atmospheric Research, 164-165, 210–225, 2015.

Cassola, F., Ferrari, F., Mazzino, A., and Miglietta, M.: The role of the sea on the flash floods events over Liguria (northwestern Italy), Geophysical Research Letters, 43, 3534–3542, 2016.

Cavaleri, L.: Wave Modeling - Missing the Peaks, Journal of Physical Oceanography, 39, 2757–2778, 2009.

15 Chawla, A., Spindler, D. M., and Tolman, H. L.: Validation of a thirty year wave hindcast using the Climate Forecast System Reanalysis winds, Ocean Modelling, 70, 189–206, 2013.

Coco, G., Senechal, N., Rejas, A., Bryan, K. R., Capo, S., Parisot, J., Brown, J. A., and MacMahan, J. H.: Beach response to a sequence of extreme storms, Geomorphology, 204, 493–501, 2014.

Corsini, S., Inghilesi, R., Franco, L., and Piscopia, R. a.: Italian Wave Atlas, Agency for Environmental Protection and Technical Services
20 (APAT), Roma, 2004.

Cox, A. T., Cardone, V. J., and Swail, V. R.: On the use of Climate Forecast System Reanalysis Wind Forcing in ocean response modeling, in: Proceedings, 12th Int. Workshop Wave, Hindcasting, Forecasting, Hawaii, USA, 2011.

De Boni, M., Cavaleri, L., and Rusconi, A.: The Italian waves measurement network, Coastal Engineering Proceedings, 1, 1992.

Dissanayake, P., Brown, J., Wisse, P., and Karunarathna, H.: Comparison of storm cluster vs isolated event impacts on beach/dune morpho-
25 dynamics, Estuarine, Coastal and Shelf Science, 164, 301–312, 2015.

Goda, Y.: Random Seas and Design of Maritime Structures, World Scientific, 1988.

Karunarathna, H., Pender, D., Ranasinghe, R., Short, A. D., and Reeve, D. E.: The effects of storm clustering on beach profile variability, Marine geology, 348, 103–112, 2014.

Lionello, P., Bhend, J., Buzzi, A., Della-Marta, P., Krichak, S., Jansà, A., Maheras, P., Sanna, A., Trigo, I., and Trigo, R.: Chapter 6 Cyclones
30 in the Mediterranean region: Climatology and effects on the environment, in: Mediterranean, edited by P. Lionello, P. M.-R. and Boscolo, R., vol. 4 of *Developments in Earth and Environmental Sciences*, pp. 325 – 372, Elsevier, 2006.

Lionello, P., Trigo, I., Gil, V., Liberato, M., Nissen, K., Pinto, J., Raible, C., Reale, M., Tanzarella, A., Trigo, R., Ulbrich, S., and Ulbrich, U.: Objective climatology of cyclones in the Mediterranean region: a consensus view among methods with different system identification and tracking criteria, Tellus A, 68, 2016.

35 Lowen, S. B. and Teich, M. C.: Estimation and simulation of fractal stochastic point processes, Fractals, 3, 183–210, 1995.

Mentaschi, L., Besio, G., Cassola, F., and Mazzino, A.: Problems in RMSE-based wave model validations, Ocean Modelling, 72, 53–58, 2013a.

Mentaschi, L., Besio, G., Cassola, F., and Mazzino, A.: Implementation and validation of a wave hindcast/forecast model for the West Mediterrenean, in: Proc of: 2th International Coastal Symposium, Plymouth, UK, 2013b.

Mentaschi, L., Besio, G., Cassola, F., and Mazzino, A.: Performance evaluation of WavewatchIII in the Mediterranean Sea, Ocean Modelling, 90, 82–94, 2015.

5 Saha, S., Moorthi, S., Pan, H.-L., Wu, X., Wang, J., Nadiga, S., Tripp, P., Kistler, R., Woollen, J., Behringer, D., Liu, H., Stokes, D., Grumbine, R., Gayno, G., Wang, J., Hou, Y.-T., Chuang, H.-Y., Juang, H.-M. H., Sela, J., Iredell, M., Treadon, R., Kleist, D., Van Delst, P., Keyser, D., Derber, J., Ek, M., Meng, J., Wei, H., Yang, R., Lord, S., Van Den Dool, H., Kumar, A., Wang, W., Long, C., Chelliah, M., Xue, Y., Huang, B., Schemm, J.-K., Ebisuzaki, W., Lin, R., Xie, P., Chen, M., Zhou, S., Higgins, W., Zou, C.-Z., Liu, Q., Chen, Y., Han, Y., Cucurull, L., Reynolds, R. W., Rutledge, G., and Goldberg, M.: The NCEP Climate Forecast System Reanalysis, Bulletin of the American
10 Meteorological Society, 91, 1015–1057, 2010.

Sartini, L., Cassola, F., and Besio, G.: Extreme waves seasonality analysis: An application in the Mediterranean Sea, Journal of Geophysical Research: Oceans, 120, 6266–6288, 2015a.

Sartini, L., Mentaschi, L., and Besio, G.: Comparing different extreme wave analysis models for wave climate assessment along the Italian coast, Coastal Engineering, 100, 37 – 47, 2015b.

15 Skamarock, W., Klemp, J., Dudhia, J., Gill, D., Barker, D., Wang, W., and Powers, J.: A Description of the Advanced Research WRF Version 3., Technical note tn-468+str. 113 pp, NCAR, 2008.

Splinder, D., Chawla, A., and Tolman, H. L.: An initial look at the CFSR Reanalysis winds for wave modeling, Technical Note, MMAB Contribution No. 290, NCEP, 2011.

Splinter, K. D., Carley, J. T., Golshani, A., and Tomlinson, R.: A relationship to describe the cumulative impact of storm clusters on beach
20 erosion, Coastal engineering, 83, 49–55, 2014.

Telesca, L. and Pereira, M.: Time-clustering investigation of fire temporal fluctuations in Portugal, Natural Hazards and Earth System Sciences, 10, 661–666, 2010.

Telesca, L., Cuomo, V., Lapenna, V., and Macchiato, M.: On the methods to identify clustering properties in sequences of seismic time-occurrences, Journal of seismology, 6, 125–134, 2002.

25 Telesca, L., Lapenna, V., Scalcione, E., and Summa, D.: Searching for time-scaling features in rainfall sequences, Chaos, Solitons & Fractals, 32, 35 – 41, 2007.

Telesca, L., Bernardi, M., and Rovelli, C.: Time-scaling analysis of lightning in Italy, Communications in Nonlinear Science and Numerical Simulation, 13, 1384 – 1396, 2008.

Tolman, H. L.: User manual and system documentation of WAVEWATCH III version 3.14, Tech. rep., NOAA/NWS/NCEP/MMAB, 2009.

30 Wadey, M. P., Haigh, I. D., and Brown, J. M.: A century of sea level data and the UK's 2013/14 storm surges: an assessment of extremes and clustering using the Newlyn tide gauge record, Ocean Science, 10, 1031–1045, 2014.